

# Clearance of group X secretory phospholipase A<sub>2</sub> via mouse phospholipase A<sub>2</sub> receptor

Yasunori Yokota, Mitsuru Notoya, Ken-ichi Higashino, Yoshikazu Ishimoto, Kazumi Nakano, Hitoshi Arita, Kohji Hanasaki\*

*Shionogi Research Laboratories, Shionogi and Co., Ltd., Sagisu 5-12-4, Fukushima-ku, Osaka 553-0002, Japan*

Received 18 September 2001; revised 30 October 2001; accepted 6 November 2001

First published online 21 November 2001

Edited by Felix Wieland

**Abstract** Given the potent hydrolyzing activity toward phosphatidylcholine, group X secretory phospholipase A<sub>2</sub> (sPLA<sub>2</sub>-X) elicits a marked release of arachidonic acid linked to the potent production of lipid mediators in various cell types. We have recently shown that sPLA<sub>2</sub>-X can also act as a ligand for mouse phospholipase A<sub>2</sub> receptor (PLA<sub>2</sub>R). Here, we found that sPLA<sub>2</sub>-X was internalized and degraded via binding to PLA<sub>2</sub>R associated with the diminished prostaglandin E<sub>2</sub> (PGE<sub>2</sub>) formation in PLA<sub>2</sub>R-expressing Chinese hamster ovary (CHO) cells compared to CHO cells. Indirect immunocytochemical analysis revealed that internalized sPLA<sub>2</sub>-X was co-localized with PLA<sub>2</sub>R in the punctate structures in PLA<sub>2</sub>R-expressing CHO cells. Moreover, in mouse osteoblastic MC3T3-E<sub>1</sub> cells that endogenously express the PLA<sub>2</sub>R, the internalized sPLA<sub>2</sub>-X was localized in lysosomes. These findings demonstrate that PLA<sub>2</sub>R acts as a clearance receptor for sPLA<sub>2</sub>-X to suppress its strong enzymatic activity. © 2001 Federation of European Biochemical Societies. Published by Elsevier Science B.V. All rights reserved.

**Key words:** Secretory phospholipase A<sub>2</sub>; Group X secretory phospholipase A<sub>2</sub>; Phospholipase A<sub>2</sub> receptor; Internalization; Clearance receptor

## 1. Introduction

Secretory phospholipase A<sub>2</sub>s (sPLA<sub>2</sub>s) are a growing family of enzymes that hydrolyze the *sn*-2 fatty acid ester bonds of glycerophospholipids to produce free fatty acids and lyso-phospholipids [1,2]. sPLA<sub>2</sub>s have several common characteristics including a relatively low molecular mass (13–18 kDa), the presence of 6–8 disulfide bridges, and an absolute catalytic requirement for millimolar concentrations of Ca<sup>2+</sup> [3,4]. At present, mammalian sPLA<sub>2</sub>s are classified into 10 different groups depending on the primary structure characterized by the number and positions of cysteine residues (IB, IIA, IIC,

IID, IIE, IIF, III, V, X and XII) [5–7]. Among them, group X sPLA<sub>2</sub> (sPLA<sub>2</sub>-X) has 16 cysteine residues located at positions characteristic of the classical types of group IB and IIA sPLA<sub>2</sub>s (sPLA<sub>2</sub>-IB and sPLA<sub>2</sub>-IIA), and also has an amino acid C-terminal extension that is typical of group II sPLA<sub>2</sub> subtypes [8]. We have recently shown that sPLA<sub>2</sub>-X is one of the enzymes that possesses a potent hydrolyzing activity toward phosphatidylcholine, a major component of the extracellular face of the plasma membrane of mammalian cells [9]. In fact, sPLA<sub>2</sub>-X can induce potent release of arachidonic acid leading to cyclooxygenase (COX)-dependent prostaglandin (PG) formation, as well as marked production of lyso-phosphatidylcholine in various cell types, including macrophages, spleen cells and colon cancer cells [10–12]. Given its high expression in macrophages and invasive colon cancers, sPLA<sub>2</sub>-X is thought to play a crucial role in the progression of various disease states, including inflammation and colon tumorigenesis, via the production of lipid mediators.

In addition to its digestive function, sPLA<sub>2</sub>-X has recently been identified as a high-affinity ligand for the phospholipase A<sub>2</sub> receptor (PLA<sub>2</sub>R) in mice [11,13]. PLA<sub>2</sub>R is a type I trans-membrane glycoprotein composed of a large extracellular portion including a characteristic tandem repeat of eight carbohydrate-recognition domains. Its overall molecular organization is related to unique members (subgroup VI) of the C-type animal lectin family, such as the macrophage mannose receptor and DEC-205 [14,15]. In the ligand–receptor relationship, there is strict species specificity, and sPLA<sub>2</sub>-IB has been identified as a high-affinity ligand of PLA<sub>2</sub>R in mice [16]. sPLA<sub>2</sub>-IIA is a relatively weaker ligand and group IID sPLA<sub>2</sub> cannot bind to PLA<sub>2</sub>R [16,17]. For the high-affinity receptor binding, proteolytic removal of the propeptide of sPLA<sub>2</sub>-X is required, being similar to the case of sPLA<sub>2</sub>-IB [13]. PLA<sub>2</sub>R is abundantly expressed in type II alveolar epithelial cells in accordance with the expression of sPLA<sub>2</sub>-IB and sPLA<sub>2</sub>-X [18]. We have recently shown that PLA<sub>2</sub>R plays a critical role in the production of pro-inflammatory cytokines during the progression of endotoxic shock by study of PLA<sub>2</sub>R-deficient mice [19,20]. As for sPLA<sub>2</sub>-IB, we have found that it elicits various biological responses via binding to PLA<sub>2</sub>R, including lipid mediator production and cell proliferation [21]. In addition, PLA<sub>2</sub>R is involved in the internalization and degradation of sPLA<sub>2</sub>-IB [22] and exogenous ligands, such as snake venom sPLA<sub>2</sub> [23].

The powerful enzymatic activity of sPLA<sub>2</sub>-X suggests that knowing about its PLA<sub>2</sub>R-mediated responses would be indispensable for understanding its physiological and pathological functions. In the present study, we found that sPLA<sub>2</sub>-X

\*Corresponding author. Fax: (81)-6-6458 0987.

E-mail address: kohji.hanasaki@shionogi.co.jp (K. Hanasaki).

**Abbreviations:** PLA<sub>2</sub>, phospholipase A<sub>2</sub>; sPLA<sub>2</sub>, secretory phospholipase A<sub>2</sub>; sPLA<sub>2</sub>-X, group X sPLA<sub>2</sub>; sPLA<sub>2</sub>-IB, group IB sPLA<sub>2</sub>; sPLA<sub>2</sub>-IIA, group IIA sPLA<sub>2</sub>; COX, cyclooxygenase; PG, prostaglandin; PLA<sub>2</sub>R, phospholipase A<sub>2</sub> receptor; Ab, antibody; CHO, Chinese hamster ovary; MEM, minimum essential medium; FCS, fetal calf serum; PBS, phosphate-buffered saline; BSA, bovine serum albumin; LAMP-2, lysosome-associated membrane protein type 2; IgG, immunoglobulin G

was rapidly internalized and degraded after PLA<sub>2</sub>R binding, thus resulting in a decrease in PGE<sub>2</sub> production. Further analysis with indirect immunofluorescent and immunoelectron microscopy revealed the transport of sPLA<sub>2</sub>-X into lysosomes after PLA<sub>2</sub>R binding, which indicates that PLA<sub>2</sub>R has a critical role as the clearance receptor for sPLA<sub>2</sub>-X.

## 2. Materials and methods

### 2.1. Materials

Sodium [<sup>125</sup>I]iodine (carrier-free, 3.7 GBq/ml) was purchased from Amersham Pharmacia Biotech. Purified recombinant mouse sPLA<sub>2</sub>-X, rabbit anti-sPLA<sub>2</sub>-X antibody (Ab), and rat monoclonal anti-PLA<sub>2</sub>R Ab (912F) were prepared as described in our previous paper [18]. The specificity of rabbit anti-sPLA<sub>2</sub>-X Ab was confirmed by its neutralizing effect on sPLA<sub>2</sub>-X enzymatic activity with no inhibitory potency against other sPLA<sub>2</sub> enzymes [9]. The specificity of 912F for PLA<sub>2</sub>R was also confirmed by a sandwich enzyme-linked immunosorbent assay (ELISA) system, in which the signal for circulating the soluble form of the receptor was absent in plasma prepared from PLA<sub>2</sub>R-deficient mice [18].

### 2.2. Comparison of sPLA<sub>2</sub>-X-induced PGE<sub>2</sub> production and the stability of sPLA<sub>2</sub>-X between PLA<sub>2</sub>R-CHO and CHO cells

Chinese hamster ovary (CHO) cells stably expressing mouse PLA<sub>2</sub>R (PLA<sub>2</sub>R-CHO cells) were prepared as described previously [11]. Human COX-2 cDNA and its expression plasmid were prepared [24] and transiently expressed in CHO and PLA<sub>2</sub>R-CHO cells with Lipofect-Amine PLUS reagent (Life Technologies) according to the instructions of the manufacturer. Cells were grown in 96-well microplates in  $\alpha$ -minimum essential medium (MEM), 10% fetal calf serum (FCS). After washing with phosphate-buffered saline (PBS), the cells were incubated with 25 nM mouse sPLA<sub>2</sub>-X in  $\alpha$ -MEM, 0.1% bovine serum albumin (BSA) at 37°C for various times. After incubation, the supernatant was collected following centrifugation at 1000  $\times$  g for 5 min at 4°C. The released PGE<sub>2</sub> was quantified with PGE<sub>2</sub> EIA Monoclonal Kit (Cayman Chemicals Co.). In separate experiments, PLA<sub>2</sub>R-CHO and CHO cells were incubated with mouse sPLA<sub>2</sub>-X for various times at 37°C. The residual PLA<sub>2</sub> activity in the supernatant was determined by chromogenic assay, as described previously [11]. Briefly, the supernatant was incubated with mixed micelles consisting of 1 mM 1,2-bis(heptanoylthio)-1,2-dideoxy-*rac*-glycero-3-phosphocholine and 0.3 mM Triton X-100 in the assay buffer containing 25 mM Tris-HCl buffer (pH 7.5), 0.12 mM 5,5'-dithiobis(2-nitrobenzoic acid), 10 mM CaCl<sub>2</sub>, 0.1 M KCl, and 1 mg/ml BSA. The reaction was monitored at the absorbance of 405 nm with a microplate reader, and the amount of the active form of sPLA<sub>2</sub>-X in the supernatant was calculated from a standard curve using intact sPLA<sub>2</sub>-X.

### 2.3. Kinetic studies on ligand internalization

Iodination of mouse sPLA<sub>2</sub>-X was performed by the chloramine T method, as described previously [22], and the specific radioactivity of <sup>125</sup>I-sPLA<sub>2</sub>-X was 1200 cpm/fmol. PLA<sub>2</sub>R-CHO cells were grown in 24-well plates in  $\alpha$ -MEM, 10% FCS. After washing with PBS, the cells were incubated with 1 nM <sup>125</sup>I-labeled mouse sPLA<sub>2</sub>-X in binding medium (Hank's balanced salt solution containing 0.1% BSA) for 2 h at 4°C. The cells were washed with PBS, resuspended in binding medium, and then incubated at 37°C. At the end of the incubation, the supernatant was removed and the cells were treated with an acidic buffer (50 mM glycine, 0.1 M NaCl, pH 3.0) for 10 min at 4°C. The acidic buffer was harvested, and its radioactivity was determined. The residual cell-associated radioactivity was determined after solubilization of the cells with 1 N NaOH. The supernatant was precipitated with 10% trichloroacetic acid, and the trichloroacetic acid-soluble and -insoluble radioactivity was determined. The specific binding was calculated by subtracting the non-specific binding obtained with 100 nM mouse sPLA<sub>2</sub>-X.

### 2.4. Analysis by indirect immunofluorescence microscopy

After incubation with mouse sPLA<sub>2</sub>-X at 37°C, the cells were washed with PBS and fixed with 4% paraformaldehyde in Na-phosphate buffer (pH 7.2) for 4 h at room temperature. After washing with PBS, the cells were permeabilized with 0.1% Triton X-100 in PBS for 15 min. They were incubated with 1% skim milk in PBS for 15 min to

block non-specific binding followed by incubation with primary Abs, including rabbit anti-sPLA<sub>2</sub>-X Ab (6  $\mu$ g/ml), rat anti-PLA<sub>2</sub>R Ab (912F, 15  $\mu$ g/ml), or rat monoclonal Ab for lysosome-associated membrane protein type 2 (LAMP-2) (ABL-93 obtained from BD Pharmingen, 2.5  $\mu$ g/ml). After rinsing with PBS, the cells were incubated with fluorescent-labeled secondary Abs, such as Alexa Fluor 488-labeled goat anti-rabbit immunoglobulin G (IgG) Ab and/or Alexa Fluor 594-labeled goat anti-rat IgG Ab (Molecular Probes, 10  $\mu$ g/ml). After washing with PBS, the coverslips were mounted with Aqua Poly/Mount (Polysciences) and viewed under a laser confocal microscope (TCS NT; Leica). Green and red indicate the localization of signals of Alexa Fluor 488 and 594, respectively.

### 2.5. Analysis by immunoelectron microscopy

After incubation with 50 nM sPLA<sub>2</sub>-X for 24 h, mouse osteoblastic MC3T3-E1 cells (ATCC) were washed and fixed in 4% paraformaldehyde in Na-phosphate buffer (pH 7.2) as described above. The cells were dehydrated in a graded series of ethanol and embedded in LR-White (London Resin). Ultrathin sections (70 nm) were mounted on collodion-treated nickel grids. The sections were allowed to react with anti-sPLA<sub>2</sub>-X Ab followed by incubation with colloidal gold (5 nm)-conjugated goat anti-rabbit IgG Ab (E-Y Laboratories). After washing, the sections were counterstained with uranyl acetate and observed under a transmission electron microscope (JEOL, JEM-1200EX).

## 3. Results and discussion

### 3.1. Comparison of sPLA<sub>2</sub>-X-induced PGE<sub>2</sub> production and the stability of sPLA<sub>2</sub>-X between PLA<sub>2</sub>R-CHO and CHO cells

In order to examine the involvement of PLA<sub>2</sub>R in sPLA<sub>2</sub>-X-induced responses, we first compared the potency of sPLA<sub>2</sub>-X for PGE<sub>2</sub> production between PLA<sub>2</sub>R-CHO cells and CHO cells. Since arachidonic acid released by sPLA<sub>2</sub>-X can be efficiently converted to PGE<sub>2</sub> via COX-2 in various cell types [10,12], human COX-2 cDNA was transiently introduced into PLA<sub>2</sub>R-CHO and CHO cells. Western blot analysis revealed that the expression level of COX-2 protein was the same between the two cell types (result not shown). In COX-2-expressing CHO cells, PGE<sub>2</sub> production elicited by exogenous arachidonic acid was markedly elevated compared to non-transfected cells and its level was comparable in the case with COX-2-expressing PLA<sub>2</sub>R-CHO cells (data not shown). As shown in Fig. 1A, sPLA<sub>2</sub>-X induced potent PGE<sub>2</sub> production in CHO cells for up to 5 h. In PLA<sub>2</sub>R-CHO cells, however, PGE<sub>2</sub> production was slightly reduced at 1 h and markedly decreased after 2 h incubation compared to CHO cells, suggesting a negative role of PLA<sub>2</sub>R on sPLA<sub>2</sub>-X functions. We then examined the residual enzymatic activity in the culture medium after incubation of the cells with sPLA<sub>2</sub>-X. As shown in Fig. 1B, active sPLA<sub>2</sub>-X mostly remained in the supernatant during the incubation for up to 24 h in CHO cells, whereas it gradually diminished from 1 h and disappeared after 24 h incubation in PLA<sub>2</sub>R-CHO cells. These findings suggest that PLA<sub>2</sub>R plays a role in the clearance of sPLA<sub>2</sub>-X resulting in the reduction of its enzymatic potency for the cell membranes.

### 3.2. Internalization and degradation of sPLA<sub>2</sub>-X via PLA<sub>2</sub>R

Next, we examined the internalization and degradation of <sup>125</sup>I-sPLA<sub>2</sub>-X after binding to PLA<sub>2</sub>R-CHO cells. After incubation with <sup>125</sup>I-sPLA<sub>2</sub>-X for 2 h at 4°C, PLA<sub>2</sub>R-CHO cells were washed, re-suspended in binding medium and incubated at 37°C for various times. After removing the supernatant, the cells were treated with acidic buffer at 4°C to dissociate the cell-surface ligand, and the residual cell-associated (acid-resis-

tant) radioactivity was determined as the intracellular ligand. As shown in Fig. 2A, most of the cell-bound ligand was removed by the acid wash before the incubation at 37°C. The amount of cell-surface ligand gradually decreased upon warming, while the intracellular radioactivity rises concomitantly, reaching a plateau after 45 min. The fate of internalized  $^{125}\text{I}$ -sPLA<sub>2</sub>-X was also examined as follows. The incubation medium after warming was subjected to trichloroacetic acid precipitation to determine the amount of native (trichloroacetic acid-insoluble) and degraded (trichloroacetic acid-soluble) ligand. As shown in Fig. 2B, about 43% of the pre-bound ligand was dissociated from the cell surface as an intact form

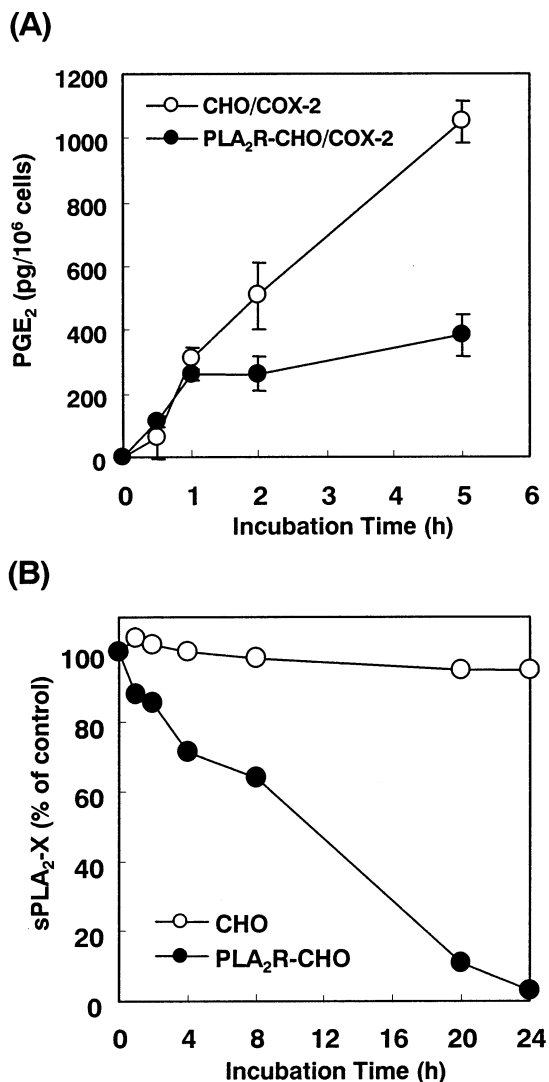


Fig. 1. Comparison of sPLA<sub>2</sub>-X-induced PGE<sub>2</sub> production and the stability of sPLA<sub>2</sub>-X between PLA<sub>2</sub>R-CHO and CHO cells. A: After transient transfection with human COX-2 cDNA, PLA<sub>2</sub>R-CHO and CHO cells were incubated with 10 nM sPLA<sub>2</sub>-X for various times at 37°C, and the PGE<sub>2</sub> amount in the supernatant was quantified. The results were expressed after subtracting the values obtained from the incubation in the absence of sPLA<sub>2</sub>-X at each time point. B: After incubation with sPLA<sub>2</sub>-X for the indicated times, the residual PLA<sub>2</sub> activity in the supernatant was measured by chromogenic assay and the amount of the active form of sPLA<sub>2</sub>-X was calculated by a standard curve using intact sPLA<sub>2</sub>-X. The results are expressed as a percentage of the amount of sPLA<sub>2</sub>-X originally added. Each point represents the mean ± S.E.M. of triplicate measurements. The data are representative of three experiments.

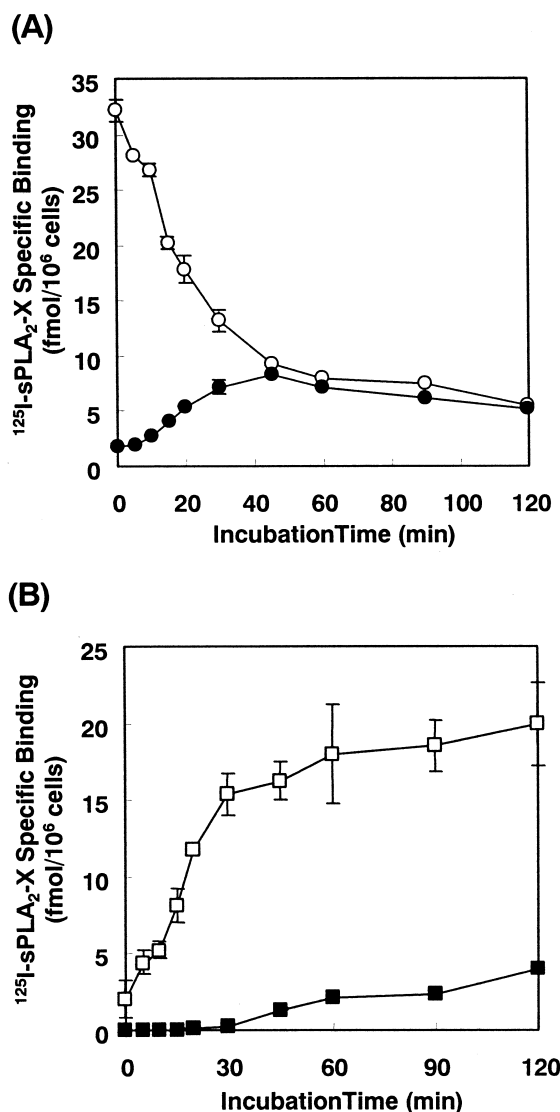


Fig. 2. Internalization and degradation of sPLA<sub>2</sub>-X in PLA<sub>2</sub>R-CHO cells. After incubation with 2 nM  $^{125}\text{I}$ -sPLA<sub>2</sub>-X for 2 h at 4°C, PLA<sub>2</sub>R-CHO cells were washed, re-suspended in binding medium and incubated at 37°C for the indicated times. After incubation, the supernatant was removed and the cells were treated with acidic buffer for 10 min at 4°C. A: The acidic buffer was harvested, and its radioactivity was determined (○). The residual cell-associated radioactivity (●) was determined after solubilization of the cells with 1 N NaOH. B: The supernatant was precipitated with 10% trichloroacetic acid, and the trichloroacetic acid-soluble (■) and insoluble (□) radioactivities were determined. The specific binding was calculated by subtracting the non-specific binding obtained with 100 nM mouse sPLA<sub>2</sub>-X from each point. Each point represents the mean ± S.E.M. of triplicate measurements. The data are representative of three experiments.

during the first 30 min of warming, which probably was due to the reversible ligand binding to the receptor. After 45 min of warming, the degraded ligands began to appear in the medium and then gradually increased. These findings demonstrate that PLA<sub>2</sub>R can internalize sPLA<sub>2</sub>-X and promote its degradation.

### 3.3. Co-localization of internalized sPLA<sub>2</sub>-X with PLA<sub>2</sub>R

In order to determine the subcellular localization of internalized sPLA<sub>2</sub>-X and PLA<sub>2</sub>R, we performed confocal immu-

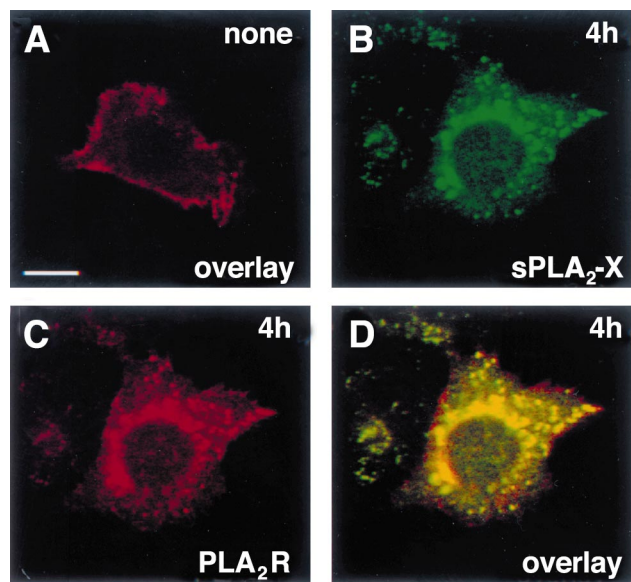


Fig. 3. Confocal microscopic analysis of subcellular localization of internalized PLA<sub>2</sub>R and sPLA<sub>2</sub>-X. PLA<sub>2</sub>R-CHO cells were incubated without (A) or with (B–D) 50 nM sPLA<sub>2</sub>-X for 4 h at 37°C. The cells were subjected to indirect immunofluorescent microscopy as described in Section 2. The red and green areas indicate the staining signals for sPLA<sub>2</sub>-X (B) and PLA<sub>2</sub>R (C), respectively, and the yellow areas indicate the regions where PLA<sub>2</sub>R and sPLA<sub>2</sub>-X are co-localized (D). Each photograph has the same magnification. The bar indicates 10 μm.

nofluorescent microscopic analysis. After incubation with sPLA<sub>2</sub>-X for 4 h at 37°C, PLA<sub>2</sub>R-CHO cells were fixed and stained with anti-sPLA<sub>2</sub>-X Ab and anti-PLA<sub>2</sub>R Ab. Before the incubation, PLA<sub>2</sub>R was mostly detected in the plasma membranes with a small portion at the intracellular punctate structures (Fig. 3A). After the incubation, sPLA<sub>2</sub>-X was internalized (Fig. 3B) and PLA<sub>2</sub>R was translocated from the cell surface to the intracellular punctate structures (Fig. 3C). The overlay of each signal revealed their co-localization in the dense perinuclear structures and the punctate cytoplasmic structures that represent the endosome, lysosomes or recycle compartment (Fig. 3D). In contrast, there were no detectable signals with both Abs under any conditions in control CHO cells (results not shown).

### 3.4. Clearance of sPLA<sub>2</sub>-X in MC3T3-E<sub>1</sub> cells

In order to verify the clearance function of native PLA<sub>2</sub>R, we examined the stability of sPLA<sub>2</sub>-X in mouse osteoblastic MC3T3-E<sub>1</sub> cells that endogenously express high levels of PLA<sub>2</sub>R [25]. In this experiment, we used polyclonal anti-PLA<sub>2</sub>R Ab that can block the association of sPLA<sub>2</sub>-X with mouse PLA<sub>2</sub>R [18]. As shown in Fig. 4, sPLA<sub>2</sub>-X activity in the culture medium gradually decreased during the incubation with MC3T3-E<sub>1</sub> cells, with the activity diminishing to 50% after 24 h-incubation. Pretreatment with anti-PLA<sub>2</sub>R Ab resulted in almost complete protection for the decline of enzymatic potency in the medium, suggesting that native PLA<sub>2</sub>R also acts as a clearance receptor for sPLA<sub>2</sub>-X.

To determine the compartmentalization of internalized sPLA<sub>2</sub>-X via native PLA<sub>2</sub>R, MC3T3-E<sub>1</sub> cells were incubated with sPLA<sub>2</sub>-X at 37°C for 24 h, and then stained with anti-sPLA<sub>2</sub>-X Ab (Fig. 5A) or Ab against LAMP-2 (Fig. 5B), a known lysosomal marker. The overlay of each signal obtained

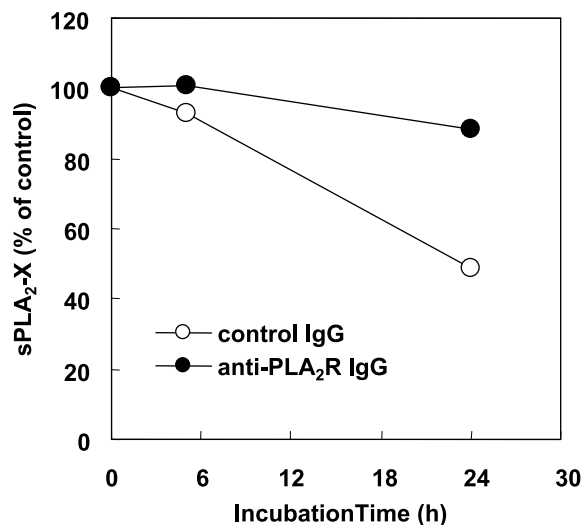


Fig. 4. Clearance of sPLA<sub>2</sub>-X in MC3T3-E<sub>1</sub> cells. MC3T3-E<sub>1</sub> cells were pre-incubated with anti-PLA<sub>2</sub>R Ab or control rabbit IgG for 1 h at 37°C, and then treated with 10 nM sPLA<sub>2</sub>-X for the indicated times at 37°C. The residual PLA<sub>2</sub> activity in the supernatant was measured and the amount of sPLA<sub>2</sub>-X was calculated. The results are expressed as the percentage of the amount of sPLA<sub>2</sub>-X originally added. Each point represents the mean ± S.E.M. of triplicate measurements. The data are representative of three experiments.

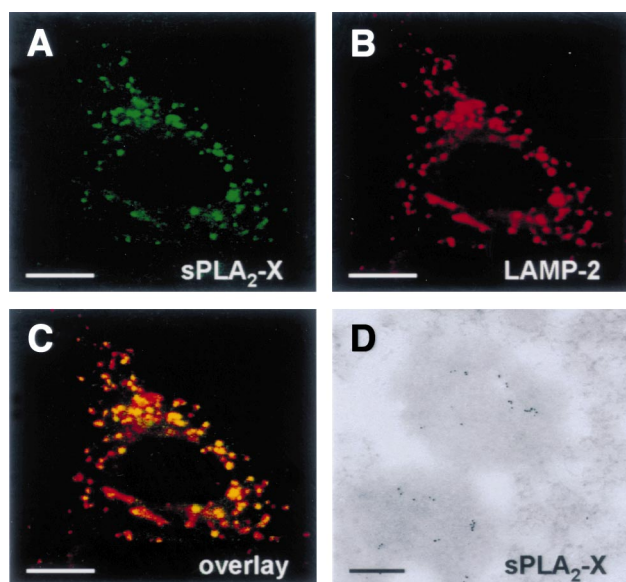


Fig. 5. Localization of internalized sPLA<sub>2</sub>-X in lysosomes. A–C: MC3T3-E<sub>1</sub> cells were incubated with 50 nM sPLA<sub>2</sub>-X for 24 h and then subjected to indirect immunofluorescent microscopy as described in Section 2. The red and green areas indicate the staining signals of sPLA<sub>2</sub>-X (A) and LAMP-2 (B), respectively. The overlay (C) shows co-localization of sPLA<sub>2</sub>-X and LAMP-2, and yellow areas indicate the regions where sPLA<sub>2</sub>-X is co-localized with LAMP-2. Each bar indicates 10 μm. D: MC3T3-E<sub>1</sub> cells were incubated with 50 nM sPLA<sub>2</sub>-X for 24 h. After fixation of the cells, ultrathin sections of the cells were reacted with anti-sPLA<sub>2</sub>-X Ab followed by incubation with colloidal gold (5 nm)-conjugated goat anti-rabbit IgG Ab. After washing, the sections were counterstained with uranyl acetate. The bar indicates 200 nm.

with confocal microscopy clearly demonstrates that the internalized ligand is transported into the lysosomes (Fig. 5C). Furthermore, analysis by immunoelectron microscopy also revealed that the colloidal gold representative of internalized sPLA<sub>2</sub>-X was localized at the lysosome-like structures (Fig. 5D). In contrast, there were no detectable signals of anti-sPLA<sub>2</sub>-X Ab in MC3T3-E1 cells without incubation of sPLA<sub>2</sub>-X (results not shown).

Endocytosis is one of the innate host defense systems against microorganisms and toxic molecules [26]. It has been noted that sPLA<sub>2</sub>-X possesses a potent hydrolyzing activity toward intact cell membranes leading to marked production of various types of lipid mediators [9]. In the present study, PGE<sub>2</sub> production by sPLA<sub>2</sub>-X was diminished by clearance of the active form of sPLA<sub>2</sub>-X in PLA<sub>2</sub>R-CHO cells (Fig. 1). Since sPLA<sub>2</sub>-X is expressed in the lung and spleen where PLA<sub>2</sub>R is co-localized in type II alveolar epithelial cells and is present in the neighboring splenic lymphocytes [18], PLA<sub>2</sub>R might act as part of the endogenous defense system by withdrawing sPLA<sub>2</sub>-X from the extracellular fluid. This could be of crucial importance in various disease states when high levels of sPLA<sub>2</sub>-X are detected, such as invasive colon cancers [12]. Although PLA<sub>2</sub>R-mediated endocytosis has been observed with other sPLA<sub>2</sub> ligands, including sPLA<sub>2</sub>-IB and snake venom sPLA<sub>2</sub> [11,13], the compartmentalization of these ligands and receptor following internalization has not been studied because of the unavailability of their specific Abs. In the present study, we identified the localization of internalized sPLA<sub>2</sub>-X and PLA<sub>2</sub>R in the vesicular structures representative for endosome, lysosomes or recycling compartment in CHO cells by confocal immunofluorescent microscopy. In the absence of sPLA<sub>2</sub>-X, PLA<sub>2</sub>R was also located at the intracellular punctate structures (Fig. 3A), suggesting a ligand-independent intracellular trafficking of the receptor as proposed for rabbit PLA<sub>2</sub>R [23]. In fact, the internalization rate constant of PLA<sub>2</sub>R for sPLA<sub>2</sub>-X ( $k_e = 0.023 \text{ min}^{-1}$ ), calculated from kinetic studies (Fig. 3), is comparable with the rates of other constitutively recycling receptors, including its structural homolog, the mannose receptor [23,27]. In MC3T3-E1 cells that express native PLA<sub>2</sub>R, the internalized sPLA<sub>2</sub>-X was transported into the lysosomes where the ligand could be degraded (Fig. 4).

In conclusion, we have demonstrated that PLA<sub>2</sub>R plays a critical role in the clearance of sPLA<sub>2</sub>-X. With respect to sPLA<sub>2</sub>-IB, PLA<sub>2</sub>R can mediate various biological responses after recognition of this ligand, including cell proliferation and lipid mediator production [21]. Recent studies have also shown that sPLA<sub>2</sub>-IB is targeted to the nucleus after its binding to the cell surface [28]. These findings suggest that sPLA<sub>2</sub>-X binding to PLA<sub>2</sub>R might be linked to some signal transduction systems leading to the induction of biological responses. Alternatively, the endosomal vesicles may serve as a vehicle delivering sPLA<sub>2</sub>-X to specific intracellular compartments where the enzyme can work before being degraded in the lysosomes. Further studies on the PLA<sub>2</sub>R-mediated endocytosis and signaling events of sPLA<sub>2</sub>-X in various tissues and

species should lead to further understanding of the physiological and pathological functions of sPLA<sub>2</sub>-X.

## References

- [1] Vadas, P. and Pruzanski, W. (1986) *Lab. Invest.* 55, 391–404.
- [2] Arita, H., Nakano, T. and Hanasaki, K. (1989) *Prog. Lipid Res.* 28, 273–301.
- [3] Tischfield, J.A. (1997) *J. Biol. Chem.* 272, 17247–17250.
- [4] Lambeau, G. and Lazdunski, M. (1999) *Trends Pharmacol. Sci.* 20, 162–170.
- [5] Six, D.A. and Dennis, E.A. (2000) *Biochim. Biophys. Acta* 1488, 1–19.
- [6] Valentin, E., Ghomashchi, F., Gelb, M.H., Lazdunski, M. and Lambeau, G. (2000) *J. Biol. Chem.* 275, 7475–7496.
- [7] Gelb, M.H., Valentin, E., Ghomashchi, F., Lazdunski, M. and Lambeau, G. (2000) *J. Biol. Chem.* 275, 39823–39826.
- [8] Cupillard, L., Koumanov, K., Mattei, M.G., Lazdunski, M. and Lambeau, G. (1997) *J. Biol. Chem.* 272, 15745–15752.
- [9] Hanasaki, K., Ono, T., Saiga, A., Morioka, Y., Ikeda, M., Kawamoto, K., Higashino, K., Nakano, K., Yamada, K., Ishizaki, J. and Arita, H. (1999) *J. Biol. Chem.* 274, 34203–34211.
- [10] Saiga, A., Morioka, Y., Ono, T., Nakano, K., Ishimoto, Y., Arita, H. and Hanasaki, K. (2001) *Biochim. Biophys. Acta* 1530, 67–76.
- [11] Morioka, Y., Saiga, A., Yokota, Y., Suzuki, N., Ikeda, M., Ono, T., Nakano, K., Fujii, N., Ishizaki, J., Arita, H. and Hanasaki, K. (2000) *Arch. Biochem. Biophys.* 381, 31–42.
- [12] Morioka, Y., Ikeda, M., Saiga, A., Fujii, N., Ishimoto, Y., Arita, H. and Hanasaki, K. (2000) *FEBS Lett.* 487, 262–266.
- [13] Yokota, Y., Higashino, K., Nakano, K., Arita, H. and Hanasaki, K. (2000) *FEBS Lett.* 478, 187–191.
- [14] Taylor, M.E., Conary, J.T., Lennartz, M.R., Stahl, P.D. and Drickamer, K. (1990) *J. Biol. Chem.* 265, 12156–12162.
- [15] Jiang, W., Swiggard, W.J., Heufler, C., Peng, M., Mirza, A., Steinman, R.M. and Nussenzweig, M.C. (1995) *Nature* 375, 151–155.
- [16] Cupillard, L., Mulherkar, R., Gomez, N., Kadam, S., Valentin, E., Lazdunski, M. and Lambeau, G. (1999) *J. Biol. Chem.* 274, 7043–7051.
- [17] Valentin, E., Koduri, R.S., Scimeca, J.C., Carle, G., Gelb, M.H., Lazdunski, M. and Lambeau, G. (1999) *J. Biol. Chem.* 274, 19152–19160.
- [18] Yokota, Y., Ikeda, M., Higashino, K., Nakano, K., Fujii, N., Arita, H. and Hanasaki, K. (2000) *Arch. Biochem. Biophys.* 379, 7–17.
- [19] Hanasaki, K., Yokota, Y., Ishizaki, J., Itoh, T. and Arita, H. (1997) *J. Biol. Chem.* 272, 32792–32797.
- [20] Yokota, Y., Hanasaki, K., Ono, T., Nakazato, H., Kobayashi, T. and Arita, H. (1999) *Biochim. Biophys. Acta* 1438, 213–222.
- [21] Hanasaki, K. and Arita, H. (1999) *Arch. Biochem. Biophys.* 372, 215–223.
- [22] Hanasaki, K. and Arita, H. (1992) *J. Biol. Chem.* 267, 6414–6420.
- [23] Zvaritch, E., Lambeau, G. and Lazdunski, M. (1996) *J. Biol. Chem.* 271, 250–257.
- [24] Hsi, L.C., Baek, S.J. and Eling, T.E. (2000) *Exp. Cell Res.* 256, 563–570.
- [25] Tohkin, M., Kishino, J., Ishizaki, J. and Arita, H. (1993) *J. Biol. Chem.* 268, 2865–2871.
- [26] Mukherjee, S., Ghosh, R.N. and Maxfield, F.R. (1997) *Physiol. Rev.* 77, 759–803.
- [27] Wiley, H.S. and Cunningham, D.D. (1982) *J. Biol. Chem.* 257, 4222–4229.
- [28] Fayard, J.M., Tessier, C., Pageaux, J.F., Lagarde, M. and Laugier, C. (1998) *J. Cell Sci.* 111 (Part 7), 985–994.